Building Simulation 2005

Ninth International IBPSA Conference
Montréal, Canada
August 15-18, 2005

NUMERICAL SIMULATION OF WATER ABSORPTION IN SOFTWOOD

Luis Candanedo and Dominique Derome
Building Envelope Performance Laboratory
Department of Building Civil and Environmental Engineering, Concordia University
Montreal, Quebec, Canada
luismiguel_78@hotmail.com, derome@alcor.concordia.ca

ABSTRACT

Whereas water can frequently come in contact with wood-based building envelope components, little work has tried to measure and model moisture uptake in orthotropic wood. This paper presents experimental results and numerical simulations of water uptake in softwood. Water absorption coefficients were measured and shown to vary according to the orientation of the fiber grain. Helium pycnometry was employed to obtain porosity values with the intention of approximating the capillary moisture content of the wood samples. From these measurements, average diffusivities were estimated. Numerical simulations of water uptake were conducted with these values and the results compared with the corresponding experimental results. Observations on the adequacy of using average diffusivities for such modeling are made.

INTRODUCTION

Building envelope systems can see their components exposed to contact with liquid water, for example cladding wetted by rain, or sheathing or structure wetted by water infiltration. In residential buildings, such components are often wood or wood-based. There have been few measurements done on the wetting of wood and, as a result, few models have been developed with the capacity to simulate moisture uptake of wood. In addition, no work so far has fully captured the impact of the three-dimensional structure of wood (Figure 1) on mass transfer and implemented it.

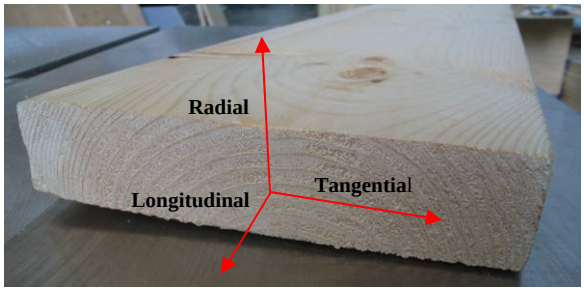

Figure 1. Directions according to the fiber grain and growth rings

Water transport in unsaturated porous materials can be studied with a variety of techniques such as nuclear magnetic resonance (NMR), gamma-ray attenuation and X-ray analysis. However, these techniques demand sophisticated and expensive equipment and qualified personnel (Krus, 1996). Researchers participating in the International Energy Agency projects have shown that using data from water absorption tests can provide a good approximation of the average liquid water diffusivity of the material (Kumaran, 1999).

This paper describes tests conducted to measure the water absorption coefficient in the longitudinal, radial and tangential directions and the capillary moisture content for one softwood species, Jack Pine. Using an equation developed by Krus and Künzel (Krus et al., 1993), average diffusivities are obtained from the measurements. The validity of using these diffusivity values in simplified numerical simulations is then ascertained by comparing the numerical results with the corresponding measurements.

After a brief summary of liquid transport in wood, the paper describes the experimental set-up and the results. Next, the simulation settings and results are provided. Finally, the results are compared and the differences discussed.

WATER TRANSPORT IN WOOD:

In order to understand liquid transport in wood, it is necessary to first examine its microscopic structure. Excellent descriptions of the wood structure of softwoods and hardwoods can be found in the works of Zimmerman (Zimmermann, 1983) and Kollmann and Côté (Kollmann and Côté, 1968). An excellent introduction to the transport of fluids in wood is found in the work by Siau (Siau, 1984).

In summary, softwoods are composed of different types of cells. The main ones for liquid transport are the tracheids that run longitudinally and that make up most of the volume of the structure.

Latewood tracheids exhibit smaller lumens or cavities than the ones in earlywood. This is explained

by the stages of growing of the trees. A smaller lumen would
mean a higher capillary pressure; therefore, water travels faster through this conduct. Fluid flow is limited by the bordered pits, which are openings connecting the cells between each other. It is important to make the distinction between permeability and capillary pressure. Permeability is many times higher in earlywood than in latewood as shown in the work by Domec and Gartner for Douglas-fir (Domec et al, 2002)

It has been recognized a Fick's type of equation cannot represent accurately moisture transport above the fiber saturation point (FSP), but this approach may provide a general description. Liquid diffusivities are not the same for wetting and drying of wood: While wetting may be simulated with a single diffusivity, the drying process can be divided into various stages (Krus and Holm, 1999). The work by Perré (Perré, 2003) on the role of wood anatomy in the drying of wood uses a percolation model for simulating fluid migration of wood.

The importance of the moisture profile has been recognized, since the moisture distribution in the wood can induce swelling creating strain gradients that can lead to cracking and warping (Plumb et al, 1985).

EXPERIMENTAL WORK

Wood samples were cut with a prismatic shape of approximate dimensions w × d × h = 40 × 40 × 50 mm³. The four vertical sides were covered with either varnish or adhesive tape. The top was left uncovered to avoid any build-up of entrapped air pressure during the water absorption which might slow down the imbibition process. Samples were suspended above a water-filled tray in such a way that the contact between their bottom surface and water was ensured (Figure 2). Their base was submerged only a few millimeters (~1-3) in order to avoid build-up of hydrostatic pressure. The environmental laboratory conditions ranged from 18 to 24°C and 50 to 70 % RH during the duration of the experiments. The water temperature was kept constant at 20°C using a constant temperature bath to avoid changes in water viscosity that might affect the absorption rate (Mukhopadhyaya et al., 2002).

Figure 2. Water uptake setup

For all the samples, their masses were recorded at various time intervals. The mass of moisture of each sample in grams was obtained by subtracting the mass of the oven dried samples from the mass of the moist samples. Finally, curves showing the cumulative weight gain versus the square root of time were plotted, and linear regression curves were computed for each. The R^2 coefficients of the fitting curves were high, ranging from 0.9734 to 0.9987. Figure 3 shows the cumulative mass as a function of the square root of time for sample A1.

The water absorption coefficient is defined by the following equation according to Schwarz (Krus et al, 1993):

$$m_W = A\sqrt{t} \quad (1)$$

where m_w is the amount of water absorbed in kg/m^2, and A is the water absorption coefficient (kg/m^{2}s$^{1/2}$). Following the definition, the water absorption coefficient A is given by the slope of the fitted curve divided by the contact area.

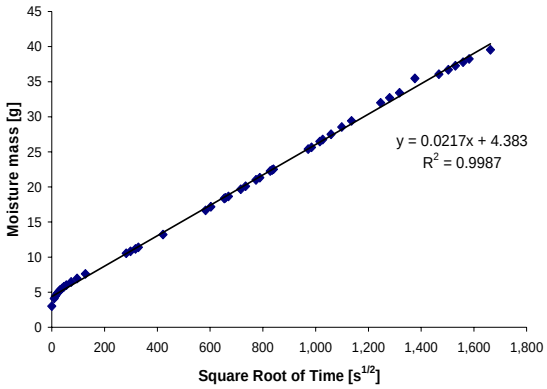

Figure 3.Cumulative mass vs square root of time for sample A1 and linear regression curve

Table 1.
Water Absorption Coefficient A

Sample	**Direction of Flow**	***A*** (kg/m^2·s$^{1/2}$)
A1	Longitudinal	0.01307
B1	Longitudinal	0.01560
C1	Longitudinal	0.01290
D1	Longitudinal	0.01339
E1	Longitudinal	0.01035
F1	Longitudinal	0.01342
E2	Longitudinal	0.01094
F2	Longitudinal	0.00998
G2	Longitudinal	0.00966
H2	Longitudinal	0.01180
A2	Radial &Tang	0.00473
B2	Radial	0.00194
C2	Tangential	0.00286
D2	Tangential	0.00265

The porosity of the samples was measured with helium pycnometry, which was preferred over mercury intrusion because the helium gas can enter smaller pores than mercury. First, the pycnometer makes a series of purges in order to remove the air and moisture entrapped in the sample. Usually the sample is subjected to a static pressure of approximately 131 to 138 kPa, or 19 to 20 psig, which allows the gas to enter the small pores of the sample. The two-chambered machine measures the gas displaced by the sample using the ideal gas law. Since the temperature, pressure and volume of the two small chambers are known the equations can be solved for the unknown volume of the sample.

Figure 4. Pycnometer AccuPyc 1330TC by Micromeritics©

From each sample, a smaller one (about 32 × 32 × 40 mm³) was taken, to be placed in the measurement cup of the pycnometer (see Figure 4). The results of the pycnometry tests are given in Table 2.

For comparison purposes, some runs were made with a mercury intrusion machine. The principle is to apply a set of increasing pressures to the sample and to measure the corresponding mercury intrusion volume. The highest reached pressure was approximately 200 MPa, or 29,000 psia. In the case of sample A1, the porosity found was 63.65 %, which, as expected, is lower than the value found by helium pycnometry.

Table 2.
Measured porosity values for each sample using helium pycnometry

Sample	Volume (cm^3)	Skeletal Volume (cm^3)	Porosity %
A1	39.74	12.12	69.49
B1	39.61	10.56	73.33
C1	40.32	12.00	70.23
D1	40.47	11.08	72.63
E1	39.44	18.91	52.05
F1	40.34	13.06	67.61
A2	40.54	13.98	65.52
B2	39.65	13.90	64.93
C2	40.47	13.90	65.66
D2	39.46	13.74	65.17
E2	39.64	11.35	71.38
F2	39.71	14.54	63.39
G2	39.66	14.08	64.50
H2	39.68	10.90	72.54

Using the equation developed by Krus and Künzel (Krus et al., 1993) that takes into account the shape of the advancing moisture front, the average value of the liquid water diffusivity in m^2/s, D, can be calculated:

$$D = \frac{\pi}{4}\left(\frac{A}{w_c}\right)^2 \quad (2)$$

where

w_c is the capillary saturated moisture content of the sample in kg/m^3, and A is the water absorption coefficient.

Assuming that w_c is equal to the density of water (1000 kg/m^3) times the porosity of the sample, the following diffusivities are obtained for sample A1: 3.31×10^{-10} m^2/s from mercury intrusion and 2.78×10^{-10} m^2/s from pycnometry.

SIMULATION - PART A

Simulation code and simulation set-up

FEMLAB uses the finite element method to solve partial differential equations. For the current simulation, the following assumptions were adopted:

- Only the liquid migration is considered; heat and water vapor transport are not taken into account. Therefore the relative humidity of the air is not taken into account.
- The material is isotropic.
- The flow is unidirectional.
- The diffusivity is constant and equal to the value obtained from the experiments.
- The boundary conditions are constant.

Two simulations were done with a 3D transient model. The first simulation used a value of diffusivity of 2.78×10^{-10} m^2/s and the second simulation a value of 3.31×10^{-10} m^2/s from the helium pycnometry and the mercury intrusion measurements, respectively.

First step:

The first step is to define the geometry of the model. A prismatic model with the same size as sample A1 was constructed (w × d × h = 0.0406 × 0.0409 × 0.0503 m³). These measurements were taken with a Vernier caliper having a reading error of ±0.05 mm.

The water uptake was taken to be in the longitudinal direction in the simulation.

Second step:

The partial differential equation (PDE) that describes the water transport must now be written.

FEMLAB incorporates a diffusion mode in which the coefficients of the equations can be input by the user.

The equation is the following:

$$\frac{\partial W}{\partial t} + \nabla \cdot (-D \cdot \nabla W) = 0 \quad (3)$$

where W is the moisture content in kg/m^3, which can also be written as $W(t,x,y,z)$, where for each coordinate t is the time. There are at least three main values of diffusivity for the direction of the unit vectors **i, j, k.** In reality, these diffusivities will be moisture content dependent, in which case the problem becomes a non-linear one. In a non-linear model, the model properties depend on the variables for which are solved (in this case, W).

This equation is a modification of the Richards equation, where the term related to the gravitational effect has been neglected since it is only is important in the presence of large cracks or holes (Roels, 2000).

Equation 3 has the same form as Fick's second law of diffusion and the heat conduction equation (Bird et al., 2002). It expresses continuity, or in other words, conservation of mass.

Third Step:

It now becomes necessary to establish the sub-domain characteristics. The sub-domain is the region bounded by the edges and vertices where the phenomenon takes place.
To do this, the values of the diffusivities for each direction must be assigned. A diagonal matrix for the diffusivities will be used:

$$D = \begin{bmatrix} a & 0 & 0 \\ 0 & b & 0 \\ 0 & 0 & c \end{bmatrix}$$

Since only the diffusivity in the z-direction is taken into account, the matrix will only have a non-zero value for the constant c.

Fourth Step:

The initial and the boundary conditions are set up.
Initial Conditions: Describe the physical state at the start of the experiment. In this experiment it is the initial moisture content.

For sample A1, the volume is 83.53 cm^3 and the initial mass of moisture is 3.0 g; the initial moisture content is calculated as $W(0)$ = 3.0 g/83.53 cm^3 = 35.91 kg/m^3 in the sub-domain, assuming that the moisture is uniformly distributed in the sample volume.

The boundary conditions may be of two types: In the *Dirichlet type*, the solution is specified on the boundary of the region, while for the *Neumann type*, the outward normal derivative dW/dn, where n is normal to the wall, is specified on the boundary (flow). The models use the Dirichlet and Neumann boundary conditions.

Assuming that all the voids are filled with water we have a value W = 694.9 kg/m^3 in the x-y plane using the porosity measurement from the pycnometer and 636.5 kg/m^3 from the mercury intrusion apparatus.

Figures 5 and 6 indicate the geometry, initial conditions and boundary conditions of simulations 1 and 2. The mass concentration at the bottom surface (z = 0) is shown in the two figures, and differences between the two correspond to the different porosities, as found using the two measurement techniques. At the other surfaces, the mass flux is set to zero.

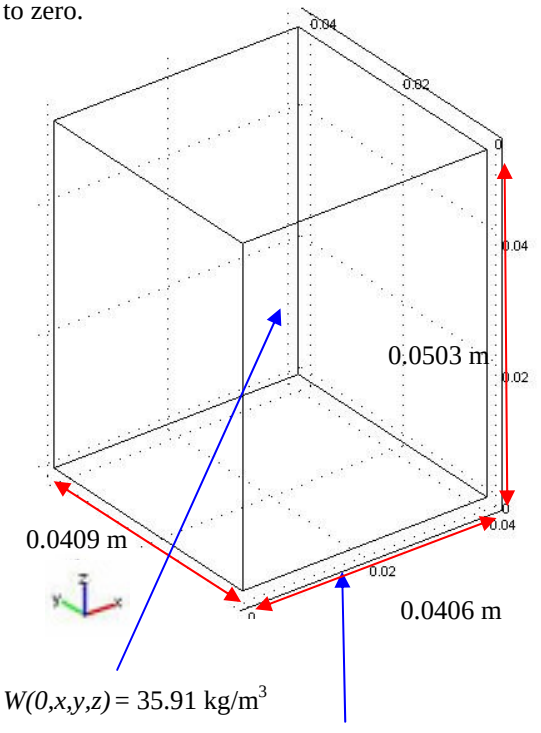

Figure 5. Geometry of the model and boundary and initial conditions for Simulation 1

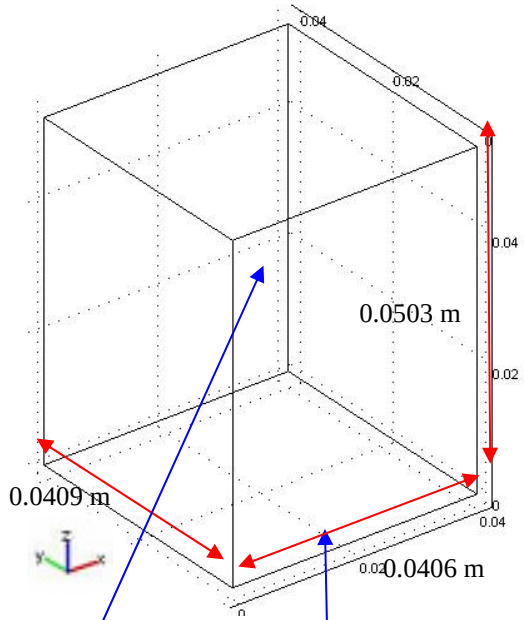

$W(0,x,y,z) = 35.91$ kg/m^3

$D = 3.31 \times 10^{-10}$ m^2/s $W(t,x,y,0) = 636.5$ kg/m^3

Figure 6. Geometry of the model and boundary and initial conditions for Simulation 2

Fifth step:

Meshing: The program automatically creates the mesh. The quantity of elements was of 3,303 for sample A1.

Time stepping: Since we have data for more than 2.7 $\times$ 10^6 seconds, a time step of 500 s was used as a time saving measure.

Sixth Step:

Simulation Results

After the program finds a solution for the specified times, a concentration gradient is obtained for the last requested time (see Figure 7). A subdomain integration of the moisture gradient or profile provides the amount of moisture at every time step desired. This integration consists of adding up the moisture contained in each of the 3,303 elements.

In a mathematical formula, this can be expressed as

$$M(t) = \sum_{i=1}^{n} V_i \cdot W_i(t) \quad (4)$$

where $M(t)$ is the total moisture in the sample at a time t, V_i is the volume of the ith finite element and $W(t)$ is the moisture content of the ith element at a time t and n is the total number of elements.

SIMULATION VERSUS MEASUREMENT RESULTS

As can be seen in Figure 8, simulations 1 and 2 yield very similar results even though the diffusivities and boundary condition values were different. As the time increases, the error diminishes. For example, during the first 16000 seconds the error is around 26%, while for the last measurement (at approximately 32 days) the error is around 6.6%.

The disparity is in part caused by the fact that diffusivity is not a constant value; it changes with the moisture content at each point. However, the approximation of an average value yields a satisfactory agreement for increasing time. It is important to remember the high level of anisotropy in wood.

A way to diminish the error is to consider two values of water absorption coefficient: an approximate coefficient for the intial 3000 s, where the absorption of water is not linear with the square root of time and the slope of the curve is steep (see Figure 3), and another once the absorption process has become linear. It must be borne in mind that physically, the diffusivity is not time dependent. It depends in factors such as temperature, materials properties and moisture content.

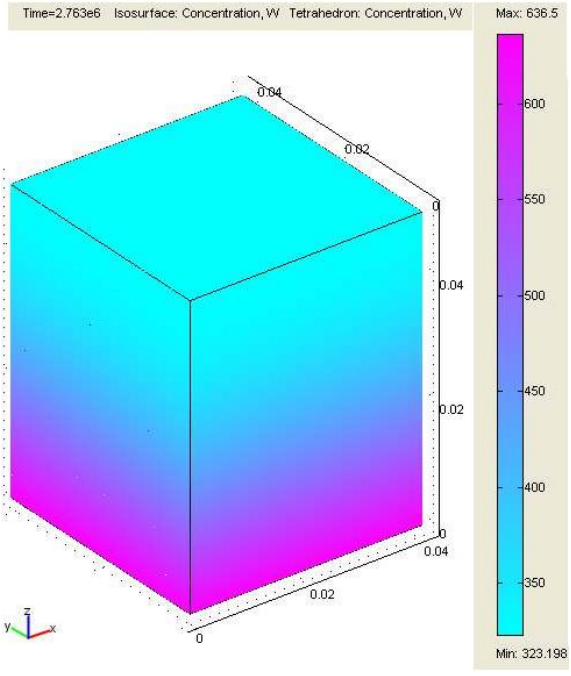

Figure 7. Concentration gradient for simulation 2 after 2.763 $\times 10^6$ s (~32 days)

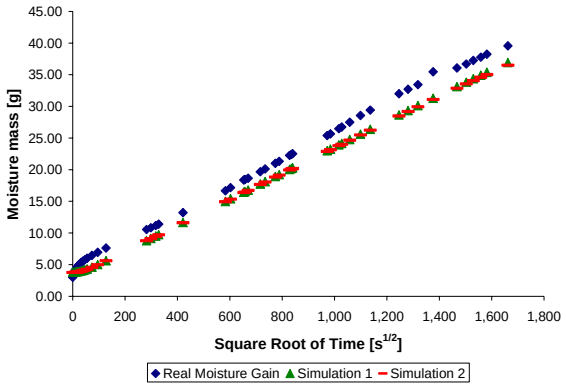

Figure 8. Comparison of experimental data with FEMLAB simulation for sample A1

SENSITIVITY STUDY ON DIFFUSIVITY

Equation (2) allows making a sensitivity analysis with respect to what a change in the diffusivity would mean in the water imbibition process.

If it is wanted to change the value of D by a factor 'x' while keeping A constant (0.01307 kg/m^{2}s$^{0.5}$), then it is necessary to change the capillary saturation moisture content. By rearranging equation (2), then:

$$w_c' = \frac{\sqrt{\frac{\pi}{4}} * A}{\sqrt{D * x}} \quad (5)$$

Evaluating the last expression for two and ten times the value of the diffusivity obtained from the porosity measurement using the mercury intrusion machine, a table for the new w_c' values is presented. (Table 3)

Table 3.
Capillary saturation moisture content neccesary to maintain the same water absorption coefficient

Times of D $D = 3.31x10^{-10}$ m^2/s	w_c' kg/m^3
2 D	450.18
10 D	201.32

The table shows that if we want to keep the same slope (A) at the beginning but having larger values for the diffusivities, it is necessary to have lower values of capillary saturation (inverse relation see equation 5). In other words, the void space has to be less so the sample gets saturated faster.

Some simulation results are presented below for different diffusivity values and boundary conditions (w_c) at the bottom of the sample.

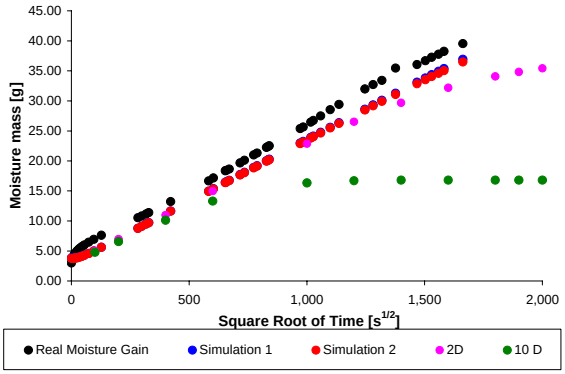

2 D = 6.62×10^{-10} m^2/s w_c = 450.18 kg/m^3
10 D = 3.31×10^{-9} m^2/s w_c = 201.32 kg/m^3

Figure 9. Simulation results for sample A1 for identical water absorption coefficient and different diffusivities and w_c values.

Knowing that the sample volume is 8.353x10^{-5} m^3, it is possible to obtain the amount of moisture at complete saturation, then for simulation 2:

$$450.18 \text{ kg/m}^3 \times 8.353x10^{-5} \text{ m}^3 = 37.6 \text{ grams.}$$

A condition which it is about to be reached in the curve of "2D".

For the "10D" simulation, the moisture content when reached a stable value would be:

$$201.32 \text{ kg/m}^3 \times 8.353x10^{-5} \text{ m}^3 = 16.81 \text{grams}$$

A condition which is reached after around 1960000 s (~23 *days).*

It is also interesting to note that at the beginning of all the simulations, the slope is the same (A coefficient) as it should be, since the parameters were fitted to eq.5.

SIMULATION - PART B

Once the average diffusivities for each orthotropic direction were determined, a very simple experiment of water absorption was carried out to compare the water content gradient and to study the adecuacy of the experimental diffusivity values.

To achieve this, a piece of wood having a prismatic shape of approximate dimensions w × d × h = 34 × 83 × 44 mm³, was glued to a glass cylinder at the top surface as shown in Figure 10.

Figure 10. Wood sample subjected to point wetting from the top.

The glass cylinder was filled with water and care was taken to keep the cylinder at least partially filled with water until the end of the experiment. Note the direction of the fiber grain. The water was mixed with commercially available food coloring to visualize the water path within the sample. After 16 days the sample was cut in half to see the water path.

The last simulation resembles simulations 1 and 2 with only changes in the geometry of the model, boundary conditions, and more importantly the diffusivity values.

The diffusivity matrix takes the following values:

$$D = \begin{bmatrix} 2.55\text{x}10^{-5} & 0 & 0 \\ 0 & 2.39\text{x}10^{-11} & 0 \\ 0 & 0 & 1.39\text{x}10^{-11} \end{bmatrix}$$

The main assumptions are:

- The material is orthotropic;
- There is point wetting;
- From the two previous points, it follows that is the flux is multidirectional;
- The diffusivities are constant and equal to the averages values from the experiments;
- The boundary condition is constant at the water-wood interface and equal to the average porosity times the density of water (670.3 kg/m^3);
- The fluxes through the other faces are zero; and
- The effect of gravity in water transport is negligible.

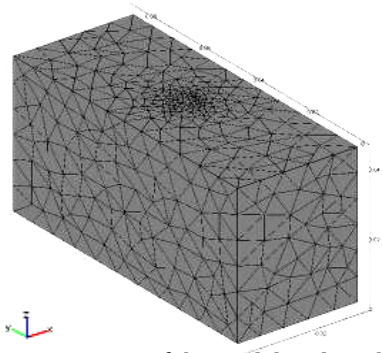

Figure 11: Geometry of the model and meshing for simulation Part B. The mesh is composed of 5839 tetrahedral elements.

SIMULATION RESULTS:

Figure 12 shows the concentration gradient for two planes .

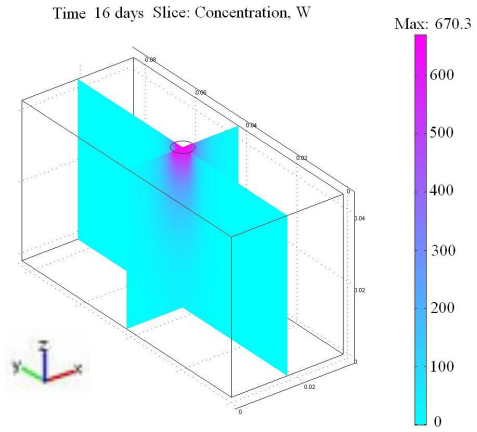

Figure 12.Calculated slice concentration gradient after 16 days of continuous wetting for z-x and y-z planes.

Figure 13 shows the sample cut in half with the corresponding water gradient obtained from the simulation. The simulation is incapable of reproducing the identical pattern of real moisture transport. Because actual moisture transport occurs preferentially (more rapidly) along the latewood rings, the simulation is incapable of reproducing the pattern exactly.

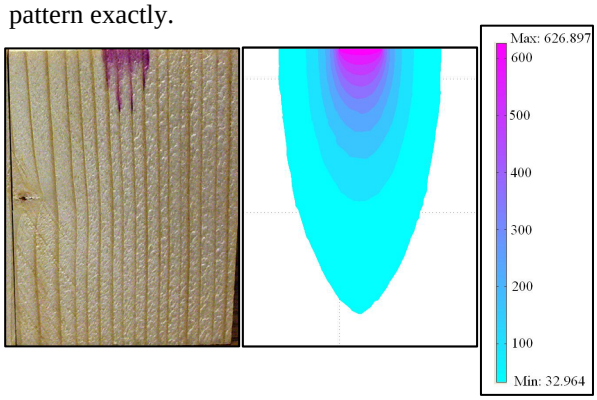

Figure 13. a) Left: The flow presents a preferential path through the latewood rings. b) Right: Isosurface concentration gradient.

CONCLUSION

This paper has shown the construction of a simplified model for simulation of an imbibition process of water in wood. The results have shown good agreement, particularly for long periods of water absorption. This means that the assumption of taking w_c equal to the porosity multiplied by the density of water is a good approximation. It is interesting to mention that even though the diffusivities and

boundary conditions were different, the results were very similar for simulations one and two.

Regarding the sensitivity study on diffusivity using equation (2), it is concluded that the only way of maitaining the same absorptivity coefficient while changing the diffusivity, it is neccesary to change the capillary saturation coefficient. The impact is reflected in a faster saturation time, but less water absorption since the capillary saturation coefficient decreases inversely to an increase in the diffusivity according to equation (5).

While the model does not reproduce the complex anatomy of wood and the preferential moisture transport path it may be an adequate approximation for building envelope applications.

Further work should include a non-linear model taking into account a moisture content dependent diffusivity. Moreover, early and latewood diffusivities should be quantified experimentally and compared to simulation.

REFERENCES

Bird, R.B., Stewart, W.E., Lightfoot, E.N. 2002. Transport Phenomena. Second Edition. John Wiley & Sons, Inc. United States of America. p 895.

Domec, J.C., Gartner, B.L. How do water transport and water storage differ in coniferous earlywood and latewood? 2002. Journal of Experimental Botany, Vol. 53, No. 379, pp 2369-2379.

Kollmann, F.P. , Côté, W.A. Principles of Wood Science and Technology I. Solid Wood. 2003. Reprinted with permission from copyright holder by CBLS. New Delhi, India. 592 p.

Krus, M. 1996. Moisture Transport and Storage Coefficients of Porous Mineral Building Materials. Theoretical Principles and New Test Methods. Fraunhofer IRB Verlag. Germany, 106 p. plus appendix.

Krus, M., Holm, A. 1999. Simple methods to approximate the liquid transport coefficients describing the absorption and drying. Proceedings of the 5th sympossium "Building Physics in the Nordic Countries', Göteborg, August 24-26. 241-248.

Krus, M., Künzel, H.M.1993. Determination of Dw from A-value. IEA Annex XXIV Report T3-D-93/02.

Kumaran, M.K. 1999. Moisture diffusivity of building materials from water absorption measurements. Journal of Thermal Envelope and Building Science, v 22, April, 349-355 p.

Mukhopadhyaya, P., Goudreau, P., Kumaran, K., Normandin, N. 2002. Effect of surface temperature on water absorption coefficient of building materials. Institute for Research in Construction, report NRCC-45369, National Reserarch Council, Ottawa, Canada. 17 p.

Perré, P. 2003. The role of wood anatomy in the drying of Wood: "Great oaks from little acorns grow". LERMAB Wood Science Laboratory. 8th International IUFRO Wood Drying Conference "Improvement and innovation in Wood Drying. A major issue for a renewable material". Brasov Romania, 11-25 p.

Plumb, O.A., Spolek, G.A., Olmstead, B.A. 1985. Heat and mass transfer in wood during drying. International Journal of Heat and Mass Transfer Pergamon Press Ltd. Vol 28, No. 9, p 1669-1678.

Roels, S. 2000. Modelling unsaturated moisture transport in heterogeneous limestone. Ph.D. thesis. Laboratory of Building Physics, Katholieke Universiteit Leuven, Leuven, Belgium, 211 p.

Siau, F.J. 1984. Transport Processes in Wood. First Edition. Springer-Verlag. Germany. p 245.

Zimmermann, M.H. 1983. Xylem structure and the ascent of sap. Springer-Verlag. Germany. 143 p.